Available online at www.sciencedirect.com
SCIENCE DIRECT®
Journal of Magnetic Resonance 176 (2005) 223–233
JMR Journal of Magnetic Resonance
www.elsevier.com/locate/jmr

Structure determination of aligned systems by solid-state NMR magic angle spinning methods

Benjamin J. Gross [a,*], Joseph M. Tanski [b], Ann E. McDermott [a,*]

[a] Department of Chemistry, Columbia University, 3000 Broadway, New York, NY 10027, USA
[b] Department of Chemistry, Vassar College, 124 Raymond Avenue, Poughkeepsie, NY 12604, USA

Received 28 April 2005; revised 14 June 2005
Available online 2 August 2005

Abstract

Single crystal rotational echo double resonance (REDOR) experiments can be used to determine the three-dimensional orientation of heteronuclear bond vectors in an amino acid, as well as the crystal's orientation relative to the rotor fixed frame (RFF). We also demonstrate that for samples uniaxially aligned along the rotor axis, the polar tilt angle of a bond vector relative to the RFF can be measured by use of an analytical expression that describes the REDOR curve for that system. These bond orientations were verified by X-ray indexing of the single crystal sample, and were shown to be as accurate as ±1°.

Keywords: Magic angle oriented sample spinning; Single crystal NMR; REDOR; Solid-state NMR; Structure determination; Biopolymers; Dipolar coupling; Oriented NMR; Heteronuclear coupling

1. Introduction

Angular or orientational constraints, when used to supplement distance constraints result in dramatically improved structure calculations for biological macromolecules [1,2]. Solution NMR and static solid-state NMR experiments involving aligned samples can be used to determine the orientation of internuclear vectors with respect to the alignment axis. Static SSNMR techniques such as the polarization inversion spin exchange at the magic angle (PISEMA) experiment have been applied to uniaxially oriented membrane proteins embedded in membranes coating stacked glass slides; and to filamentous bacteriophage samples magnetically aligned in solutions of low enough mobility to be treated by NMR as solids [3,4]. Two-dimensional PISEMA/PISA analysis is then used to determine structures of protein backbones, with emphasis on the example of amide $^{1}H^{15}N$ bonds in α-helices, and determination of helical tile angles relative to the alignment axis (B_0 axis). Although complexities regarding corrections for motional dynamics have been debated in the literature [5], and development of new techniques of this type is still an ongoing effort, it is important to note that several PDB entries have already appeared that are largely based on the PISEMA/PISA method [6–8]. A small degree of orientation can be induced in a solution sample via the effect of a strong electric or magnetic field on an aligning media or the sample itself if sufficient anisotropic magnetic or electric susceptibility exists. A solute under either condition can have an order parameter of less than 1% due to incomplete motional averaging by way of slightly anisotropic molecular tumbling, which is a sufficient degree of alignment for oriented solution NMR experiments [9–13]. This approach has had tremendous impact on the quality of solution NMR structures.

A third and highly analogous approach involves aligned samples for magic angle spinning experiments [14]. In brief, dipolar recoupling experiments applied

* Corresponding authors. Fax: +1 212 932 1289 (A.E. McDermott).
E-mail addresses: bjg30@columbia.edu (B.J. Gross), aem5@columbia.edu (A.E. McDermott).

1090-7807/$ - see front matter © 2005 Elsevier Inc. All rights reserved.
doi:10.1016/j.jmr.2005.06.008

to aligned samples provide orientational information, in contrast to measurements on powdered samples that are generally used to provide distance constraints. Thus, it is possible to have the best of both worlds, and reclaim the information lost under MAS while maintaining high chemical shift resolution. Great strides have been made in assignments of uniformly enriched proteins by solid-state NMR methods [15–17], thus it is appropriate to review the possibilities of MAOSS experiments in the context of uniformly isotopically enriched samples. Such experiments should, in principle, obviate the need for laborious repetitive experiments with specifically labeled samples, and are not limited to the identification of a single structural feature. Experiments performed during MAS of a uniaxially aligned solid sample (magic angle oriented sample spinning—MAOSS) can provide constraints based on orientations of individual dipolar and/or CSA tensors with orientations defined in the rotor fixed frame [14,18].

The rotational echo double resonance (REDOR) experiment [19] selectively recouples heteronuclear spin pairs during MAS thereby allowing for measurement of that pair's dipolar coupling frequency (ω_D). In a powder sample, ω_D can be used to extract the distance between nuclei, for example, ^{13}C–^{15}N distances from 1 to 6 Å [20], while in a uniformly aligned sample ω_D can be used to determine internuclear orientation. The REDOR experiment is a key candidate as a general method for determining orientational constraints based on ^{13}C–^{15}N backbone vectors as both the α and the carbonyl carbons of every peptide backbone are connected to a single nitrogen atom [18]. The ^{13}C–^{15}N distances in a protein backbone are essentially invariant, and therefore extracting orientations is relatively straightforward. Application of this technique on a sample that is uniaxially aligned along the axis of a MAS rotor can result in the measurement of ω_D over all azimuthal internuclear vector orientations (ϕ^{RFF}), allowing for the unique determination of the internuclear distance r_{CN} and the internuclear vector's polar tilt angle (θ^{RFF}) in the rotor fixed frame of reference (RFF). Taken a step further, a single crystal sample yields a dipolar coupling measurement specific to the internuclear distance and both polar and azimuthal angles of the bond vector in the RFF. This is the ultimate REDOR measurement of the spatial variables, wherein the dipolar coupling frequency ($\omega_D(r, \theta^{RFF}, \phi^{RFF})$) can be used to constrain the complete three-dimensional spatial orientations of bond vectors. These data would be invaluable as constraints in an overall protein structure determining calculation.

To demonstrate the potential of a dipolar coupling measurement of an ordered sample, REDOR experiments were performed on a single crystal of the model compound L-alanine (uniformly labeled ^{13}C, ^{15}N). It was demonstrated that the complete orientation of the C_α–N bond vector could be determined by a global curve fitting scheme of the REDOR data. The single crystal sample was also used to simulate a REDOR experiment of a uniaxially oriented sample by summation of the data acquired over numerous orientations, which were then fit to an analytical model derived herein. Both methods have potential use in collecting orientational constraints in single crystal and uniaxially aligned protein systems.

2. Experimental

2.1. Sample

A mixture of 10% uniformly labeled L-alanine (U, ^{13}C, ^{15}N) and 90% natural abundance L-alanine was recrystallized from deionized water (>18 MΩ cm^{-1}) taken from a HYDRO Picosystem. Large (~6 mm^3) and small crystals were grown in this fashion over the course of several days. The smaller crystals were crushed, using a mortar and pestle into powder sample, while the larger crystals were set aside for use in the single crystal experiments. The dilution of isotopically enriched species prevented unwanted effects of long-range, intermolecular nuclear couplings.

A large (~5 mm^3) L-alanine crystal was encased in a silicone rubber (Dow Corning, Sylgar 184 Elastomer Kit) support inside of a 4 mm standard MAS rotor (Varian). The crystal was loaded into the sample rotor, which was then filled with a dimethyl-siloxane/polymerizing catalyst mixture. The polymerization process solidified the poly-dimethyl-siloxane (PDMS), molding it to the inside of the rotor. The cylindrical shaped polymer-encased crystal block, shown schematically in Fig. 1A, could then be removed and reinserted into the rotor freely with the crystal's orientation relative to the rotor being preserved. This portability conveniently allows for the crystal orientation to be verified by X-ray indexing.

2.2. X-ray

The cylindrical polymer-crystal block was taken from the rotor and loaded into a Bruker single crystal X-ray diffractometer (with CCD detector), with the vertical axis of the cylinder coincident to the vertical axis of instrument's goniometer. Since the polymer cylinder holding the alanine crystal is amorphous and thus will not scatter the X-ray radiation in any coherent fashion, it had no anticipated effect on the collected data. The unit cell parameters were readily identified to within reasonable accuracy as compared to literature values [21,22]. The data for the diffractometer was then used to identify the orientations of the unit cell axes (Table 1) and verify the literature unit cell parameters showing $P_{2_12_12_1}$ symmetry (Fig. 1B). Because the vertical

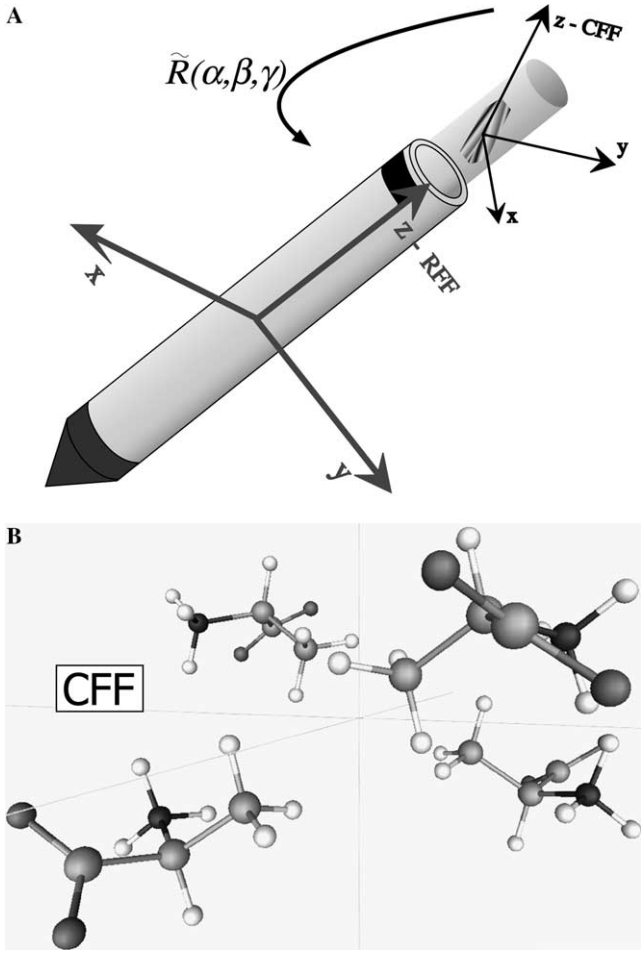

Fig. 1. (A) The spatial frame transformation of the dipolar vector to the laboratory frame from the crystal fixed frame (denoted CFF) and the rotor fixed from (denoted RFF) is depicted here in this representation of the single crystal L-alanine sample in a MAS sample rotor. (B) The unit cell of L-alanine exhibits $P_{2_12_12_1}$ symmetry containing the four distinct orientations per cell observed in the orientationally dependent REDOR experiments. The four orientations of the unit cell are related to one another by a 180° rotation about the crystallographic axis that separates each species in the x–y plane. These transformations are mathematically defined by Eq. (7).

axes of the goniometer, the polymer cylinder, and the MAS rotor were all coincident, these data directly represent the orientation of the L-alanine crystal's unit cell in the frame of reference defined by the MAS rotor. These data verify the relation to the frame of reference defined by the sample rotor (RFF), and the frame of reference defined by the crystallographic axes, or crystal fixed frame (CFF). The sample was then reloaded into the MAS sample rotor for analysis by SSNMR.

2.3. SSNMR

SSNMR spectroscopy was performed using a Varian InfinityPlus 400, triple resonance instrument, with a T3 triple resonance, 4 mm MAS probe in a $^{1}H/^{13}C/^{15}N$ configuration. Carrier frequencies were set to 396.7750, 99.7785, and 40.2065 MHz, respectively. The powder sample was center packed (central 6 mm) in a 4 mm standard rotor. The single crystal/polymer block sample was similarly packed in the center of the rotor for maximum field homogeneity. All of the performed REDOR experiments employed a pulse sequence shown schematically in Fig. 2, which was largely based on the

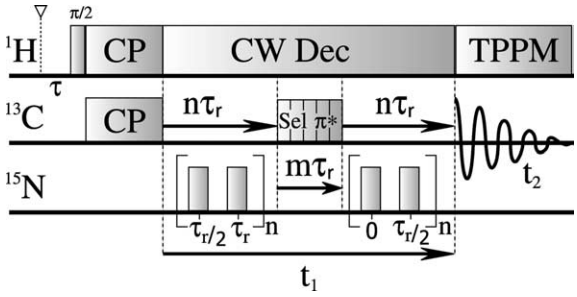

Fig. 2. The pulse sequence for the ^{13}C detected, orientationally dependent 2D REDOR experiment used throughout this study. The pulse sequence is initiated by a trigger signal (∇) from the spin speed controller maintaining consistency in the initial azimuthal orientation between acquisitions. After an adjustable delay period (τ) the RF pulsing commences.

Table 1
Collected distance and angular measurements from X-ray and neutron diffraction, and single crystal and uniaxially oriented REDOR NMR methods

	Indexing	X-ray diffraction	Neutron diffraction	Single crystal global curve fit	Uniaxial sample fit
$^{13}C_\alpha{}^{15}N(\theta^{CFF},\phi^{CFF})_1$		48.8°, 165.1°	48.7°, 165.0°	48.7°, 165.0°	—
$^{13}C_\alpha{}^{15}N(\theta^{CFF},\phi^{CFF})_2$		48.8°, −14.9°	48.7°, −15.0°	48.7°, −15.0°	—
$^{13}C_\alpha{}^{15}N(\theta^{CFF},\phi^{CFF})_3$		131.2°, 194.9°	131.3°, 195.0°	131.1°, 195.0°	—
$^{13}C_\alpha{}^{15}N(\theta^{CFF},\phi^{CFF})_4$		131.2°, 14.9°	131.3°, 15.0°	131.3°, 15.0°	—
α	114.7°			119.7°	—
β	35.3°			35.5°	—
γ	—			189.7°	—
$^{13}C_\alpha{}^{15}N(\theta^{RFF},\phi^{RFF})_1$				32.6°, 255.3°	31.7°, —
$^{13}C_\alpha{}^{15}N(\theta^{RFF},\phi^{RFF})_2$				76.7°, 23.6°	76.0°, —
$^{13}C_\alpha{}^{15}N(\theta^{RFF},\phi^{RFF})_3$				115.1°, 223.8°	116.3°, —
$^{13}C_\alpha{}^{15}N(\theta^{RFF},\phi^{RFF})_4$				130.4°, 97.7°	126.1°, —
r		1.501 Å	1.487 Å	(1.505 Å)	(1.505 Å)

J-decoupled REDOR experiment of Jaroniec et al. [23]. The Gaussian selective chemical shift refocusing π-pulse Jaroniec used was replaced with a DANTE pulse train due to equipment constraints. Proper phase cycling resulted in complete removal of all resonances not selected by the DANTE pulse train. The more significant modification to the pulse sequence is the addition of the external trigger for sequence initiation. The tachometer signal of the sample spinning speed controller was used as a triggering source to maintain a consistent initial rotational coordinate of the sample rotor throughout the course of signal averaging.

Sample spinning speed was maintained at 10 kHz resulting in a rotor period of 100 μs. Six separate experiments were performed with an incrementally adjusted delay between the trigger and the start of the pulse sequence by 10 μs. This yielded a series of measurements varied by a stepwise adjustment of the initial azimuthal angle of the rotor from 0 to π by increments of π/5. The REDOR evolution progressed in increments of four rotor periods per data point to a total acquisition length of 38 ms. The ^{15}N REDOR π-pulses were applied for a duration of 11 μs at half rotor intervals to generate the dipolar reduced signal (S_r). The DANTE pulse train consisted of 20 pulses of 0.5 μs duration separated by a 211 μs delay for appropriate selection of the $^{13}C_\alpha$ chemical shift. To occupy an integer number of rotor periods, delays of appropriate, minimal length were added before and after the DANTE sequence, the totality of which occupied ~4.8 ms.

Repeating the synchronously triggered experiment over 70 evenly spaced orientations simulated uniaxial alignment. Simulation (not shown) revealed that a number of orientations significantly higher than 70 did little to improve spectral quality at the experimental acquisition length. A number significantly smaller than 70 caused added features to appear, similar to those seen in a simulation of a truncated signal.

For the powder experiments, the synchronizing trigger was removed and the ^{15}N REDOR π-pulses were 19.5 μs long. The experiments were otherwise identical.

2.4. Processing

All spectra were processed by custom programs written for GNU Octave (2.1.50-11) [24] on an Apple G4 Powerbook running OS X. Exponential line broadening was applied to the direct detect dimension before applying a fast Fourier transform (FFT) algorithm. The successive C_α peaks (in the CS dimension) were integrated by summation to create the reduced (S_r) and standard (S_0) REDOR signals. They were then combined to generate the REDOR curve ($\Delta S/S_0$), to which Gaussian line broadening was applied prior to FFT, generating the dipolar coupling spectra.

The six single crystal dipolar spectra were each fit to four pairs of Gaussian peaks, each pair symmetric about zero with their respective separations all defined as $\omega_d(r, \theta_i^{RFF}, \phi_i^{RFF})$. All six spectra were simultaneously fit to orientational coordinates defined by the same values of (θ^{CFF}, ϕ^{CFF}) and Euler rotation angles α, β, and γ_0 which define the frame of reference transformation between the CFF and RFF depicted in Fig. 1A. The difference between the experimental data and the curve fit simulations was minimized using the 'fmins' program provided by GNU Octave-Forge. In a similar fashion, the simulated uniaxially oriented sample data was fit in the frequency domain to Eq. (13) after spectral processing similar to the single crystal experiments.

3. Results and discussion

The X-ray diffraction data for a single crystal of L-alanine was used to index the orientations of the crystallographic axes relative to the axis of its cylindrical polymer encasing. Because the axis of the polymer cylinder was coincident with the axis of the sample rotor, the X-ray indexing data provided the information necessary to generate the rotation matrix $\tilde{R}$, defining the CFF to RFF transformation. The Cartesian coordinates of the crystallographic axes (a, b, c) became the rows of the inverse rotation matrix $\tilde{R}^{-1}$, which can transform directional vectors from the CFF to the RFF

$$\tilde{R}^{-1} = \begin{pmatrix} a_x & a_y & a_z \\ b_x & b_y & b_z \\ c_x & c_y & c_z \end{pmatrix}. \quad (1)$$

For matrix element m_n, m is the unit cell axis and n indicates the RFF axis to which that coordinate belongs. The inverse (or the transpose) of this matrix gives the rotation matrix $\tilde{R}$, from which the Euler angles (α, β, and γ) are extracted using the standard method. Note that γ could not be independently determined at this step as the rotational position of the polymer/crystal block in the diffractometer may not have been the same as in the sample rotor, relative to the triggering point of the pulse sequence (∇). The value of γ will be extracted by fitting the REDOR data in a later step. The structural coordinates of L-alanine given in the CFF were taken from literature values. From these data, the complete structural three-dimensional orientation of the single crystal of L-alanine to be used for SSNMR is confirmed, providing independent verification of the REDOR results.

In the generic REDOR experiment, a chemical shift echo is performed on the detection, or primary channel. Dipolar recoupling is achieved by a series of rotor-synchronized π-pulses (spaced at half rotor intervals) applied to the secondary channel over the course of the chemical shift echo (^{13}C and ^{15}N channels, respectively). This prevents complete refocusing of the dipolar

coupling component of the Hamiltonian, and causes a time dependent dephasing of the signal, reflective of the orientationally dependent average dipolar coupling frequencies. The expression for the REDOR signal, of a single dipolar coupling vector orientation, described in the RFF is given as

$$\frac{\Delta S}{S_0} = 1 - \cos(n\tau_r \bar{\omega}_{\mathrm{D}}) = 1 - \cos\left(4\sqrt{2} n\tau_r D \sin\theta^{\mathrm{RFF}} \cos\theta^{\mathrm{RFF}} \sin\phi^{RFF}\right), \quad (2)$$

where

$$D = \frac{\mu_0}{4\pi}\frac{\gamma_I \gamma_S \hbar}{2\pi r^3}. \quad (3)$$

This model works under the guise of a two-spin system as additional, proximal spins will convolute the dephasing process with additional dipolar frequencies. Experimentally, this requires site specific labeling and often dilution of the sample with natural abundance material. To perform this analysis on a, generally more appealing, uniformly labeled sample, a degree of selectivity was introduced into the pulse sequence. A selective CS refocusing pulse was employed on the ^{13}C channel and the extraneous (unflipped) resonances were eliminated over the course of phase cycling (selective π-pulse $= xy\bar{x}\bar{y}$, receiver $= x\bar{x}x\bar{x}$). This is the heart of the *J*-decoupled REDOR sequence by Jaroniec et al., which allows for the use of a singly labeled ^{15}N, uniformly labeled ^{13}C sample in these REDOR experiments [23]. It has been shown that one could apply selective pulses to both the ^{13}C and ^{15}N channels for REDOR experiments on a uniformly ^{15}N and ^{13}C labeled sample [25], but was unnecessary in these experiments as only one ^{15}N moiety was present.

A soft Gaussian pulse was used in [23], but a DANTE pulse train [26] was sufficiently selective, and can be performed on more generally available hardware. This is the pulse sequence described in Fig. 2, and used throughout this study. The DANTE sequence is a series of hard, small angle pulses that are spaced by delays commensurate with the period of the desired chemical shift resonance. The pulses are applied as the CS moiety refocuses along the pulsing axis, tipping it stepwise further towards a complete π rotation. This serves to eliminate the other signals as they become further dephased and are lost over the course of the experiment, thus isolating the signal of the desired chemical shift resonance. This isolation allows for employing the two-spin analytical expressions based on Eq. (2) to a multi-spin system.

In the case of a uniquely ordered sample, such as a single crystal, Eq. (2) is a sufficient definition for the REDOR signal ($\Delta S/S_0$). As shown in Fig. 3B, a Fourier transform of this curve gives a pair of singularities at $\pm\bar{\omega}_{\mathrm{D}}$ indicating one set of orientation coordinates $(r, \theta^{\mathrm{RFF}}, \phi^{\mathrm{RFF}})$. For a distribution of orientations it is possible to describe the dipolar spectra with an appropriate integral. In the case of an isotropic powder sample one must integrate over all possible orientations

$$\frac{\Delta S}{S_0} = 1 - \int_0^{\pi}\int_0^{2\pi} \cos(4\sqrt{2} n\tau_r D \sin\theta\cos\theta\sin\phi) \times \mathrm{d}\phi \sin\theta \,\mathrm{d}\theta. \quad (4)$$

While a numerical analysis of Eq. (4) is achievable using computer simulations, an analytical solution eases the difficulty and expense of such calculations. In an effort to avoid of the difficulties of integrating trigonometric functions of trigonometric functions, an analytic expression was developed by Mueller [27] based on Bessel functions of the first kind. Integrating Mueller's expression over a powder average yields a final analytical expression that is solely distance dependent. This equation is universally descriptive of two-spin REDOR type measurements of powder samples

$$\frac{\Delta S}{S} = 1 - \left[J_0\left(\sqrt{2} n\tau_r D\right)\right]^2 + 2\sum_{k=1}^{\infty}\frac{1}{16k^2-1} \times \left[J_k\left(\sqrt{2} n\tau_r D\right)\right]^2. \quad (5)$$

$J_k(x)$ is a Bessel function of the first kind of order k. In a fit of this data to the REDOR curve (as a function of time), D (proportional to $1/r^3$) is the only unknown. Fig. 3F displays that a Fourier transform of the signal would yield a powder pattern centered on zero. While the width of this spectrum is indicative of the dipolar coupling constant, and thus the internuclear distance, a more accurate fit can be made of the time dimension data. Curve fitting the REDOR signal, measured on a powder sample, to Eq. (5) yields the internuclear distance of the dipole pair.

To interpret the single crystal L-alanine REDOR data, a stepwise elimination of variables is necessary to simplify the analysis. The first step is to identify the distance between the ^{13}C and ^{15}N nuclei. To this end the modified *J*-decoupled REDOR experiment was performed on the powder L-alanine sample. Fig. 4 shows the 1D ^{13}C MAS spectrum of the L-alanine sample as well as a curve fit of the C_α resonance REDOR data to Mueller's model truncated at $k = 5$, and modified to reflect the impact of long duration ^{15}N π-pulses relative to the rotor period

$$\frac{\Delta S}{S} \cong 1 - \left[J_0\left(\sqrt{2} n\tau_r D\frac{\cos((\pi/2)\varphi)}{1-\varphi^2}\right)\right]^2 + 2\sum_{k=1}^{5}\frac{1}{16k^2-1} \times \left[J_k\left(\sqrt{2} n\tau_r D\frac{\cos((\pi/2)\varphi)}{1-\varphi^2}\right)\right]^2, \quad (6)$$

with $\varphi = 2\tau_p/\tau_r$, where τ_p is the π-pulse duration [28]. This is a pertinent correction factor as high speed MAS would be required for chemical shift resolution of a biological macromolecule. The short rotor period,

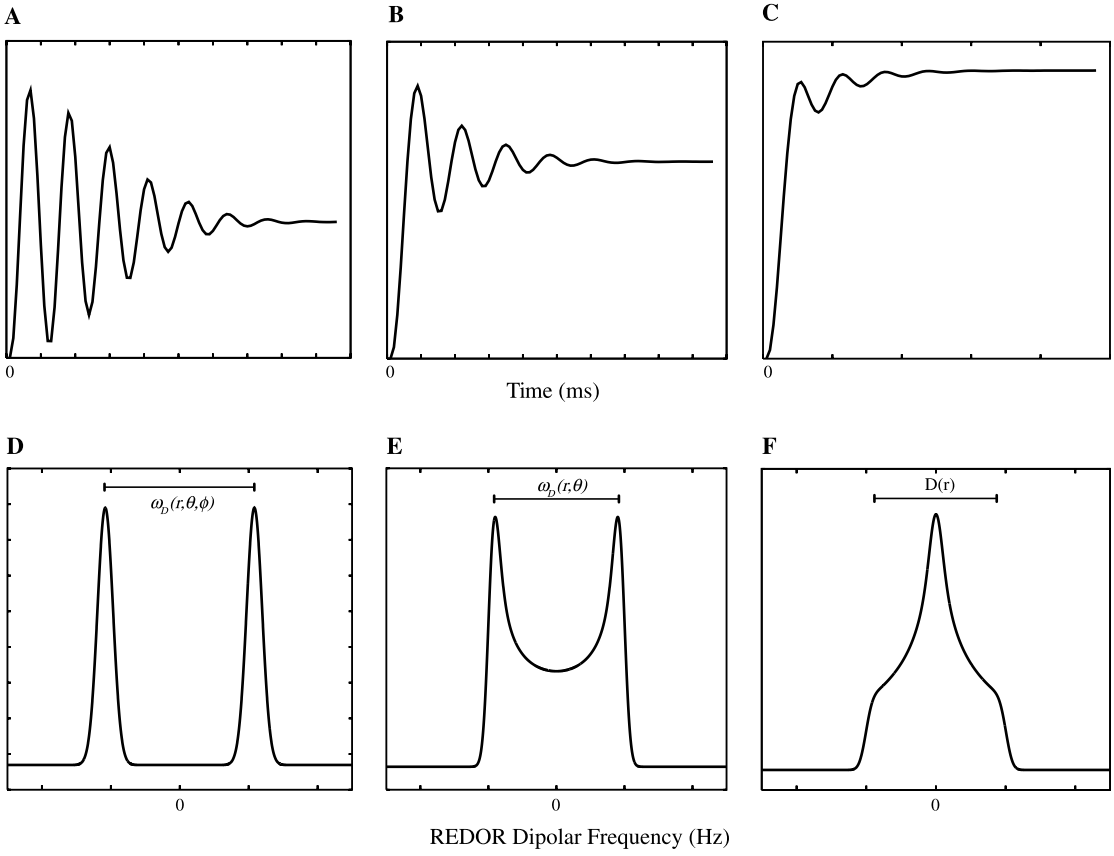

Fig. 3. Comparison of simulated REDOR data over different sample morphologies show what type of spectra to expect and indicate which analysis method is most prudent. (A,D) Depict the time and frequency domains (respectively) of the REDOR measured, heteronuclear coupling frequency of a single internuclear vector orientation best suited for analysis by frequency domain peak separation. (B,E) Similarly depict the REDOR time and frequency domains for a uniaxially oriented array of orientations also best analyzed by peak splittings, while (C,F), respectively, show REDOR time and frequency domains of a powder distribution best analyzed by time-domain curve fitting.

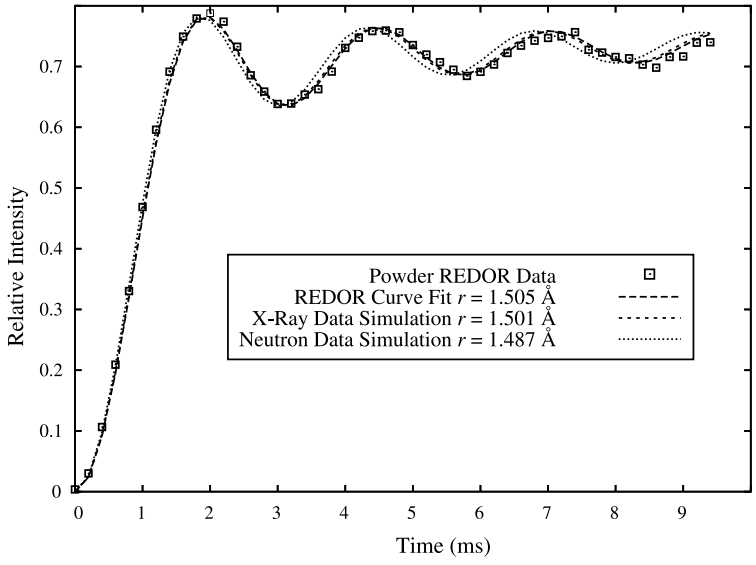

Fig. 4. The ^{13}C–^{15}N REDOR curve of the α carbon in the L-alanine powder sample fit to Eq. (6) (dashed line). The curves generated by the X-ray and neutron diffraction values for r are also shown for comparison.

and sample and equipment constraints on the applied power of an RF pulse, force a ^{15}N π-pulse duration (φ) on the order of 20–40% of the rotor period. A best-fit analysis of the L-alanine data to Eq. (6) yields an internuclear distance of 1.505 Å. The X-ray diffraction data in [22] gives a C_α–N internuclear distance of 1.501 Å and the neutron diffraction data of [21] gives 1.487 Å. This slight disagreement is commensurate with prior studies indicating that dipolar couplings measured by solution or solid-state NMR typically correspond to slightly (0.5–3%) longer distances than those measured by X-ray or neutron diffraction [29,30]. With r being solved, the remaining variables are the orientation parameters.

There are a number of conventions available in terms of how to define the orientation parameters of the internuclear bond vector. Being that the measurement is defined in the RFF, it would immediately seem practical to simply define the bond vector orientation in terms of RFF spherical polar coordinates ($\theta^{\mathrm{RFF}}, \phi^{\mathrm{RFF}}$). However, since L-alanine conforms to a $P_{2_12_12_1}$ packing motif, there are four unique orientations present per unit cell. This leads to four individual sets of RFF coordinates giving a total of eight variables defining the final dipolar spectrum. This approach is seen to be impractical when one considers that each dipolar coupling value is dependent on θ_i^{RFF} and ϕ_i^{RFF}. Not knowing either coordinate results in a family of possible solutions for each spectral peak pair.

Another option is to define the geometric parameters in the CFF and relate those to the RFF by the frame transformation ($\tilde{R}$) in a similar way as the X-ray data was presented. At first glance, this complicates matters by adding the three Euler angles as variables. Fortunately, the $P_{2_12_12_1}$ crystal packing motif is highly symmetric, and, as displayed in Fig. 1B, is characterized by each of the four moieties undergoing a 180° rotation around the axis that separate each species from its neighbor. One can employ the following operations to relate the four orientations (using Cartesian coordinates)

$$S_1 = \begin{pmatrix} 1 & 0 & 0 \\ 0 & 1 & 0 \\ 0 & 0 & 1 \end{pmatrix} \quad S_2 = \begin{pmatrix} -1 & 0 & 0 \\ 0 & -1 & 0 \\ 0 & 0 & 1 \end{pmatrix}$$
$$S_3 = \begin{pmatrix} -1 & 0 & 0 \\ 0 & 1 & 0 \\ 0 & 0 & -1 \end{pmatrix} \quad S_4 = \begin{pmatrix} 1 & 0 & 0 \\ 0 & -1 & 0 \\ 0 & 0 & -1 \end{pmatrix}. \tag{7}$$

To generate the four orientations in the CFF one only need apply the appropriate symmetry operator S_i to the CFF bond vector

$$\vec{v}(\theta,\phi)^i = S_i\vec{v}(\theta,\phi). \tag{8}$$

Following suit with the frame transform ($\tilde{R}(\alpha,\beta,\gamma)$) gives the four orientations defined as follows

$$\vec{v}(\theta_i^{\mathrm{RFF}},\phi_i^{\mathrm{RFF}}) = \tilde{R}S_i\vec{v}(\theta^{\mathrm{CFF}},\phi^{\mathrm{CFF}}). \tag{9}$$

Using Eq. (9), it is possible to define all four experimental dipolar coupling orientations with two directional coordinates, the predefined symmetry operations, and the Euler rotation angles for frame transform. If one assumes the preexisting determination of the unit cell symmetry ($P_{2_12_12_1}$), then there are only five variables to be identified ($\alpha,\beta,\gamma,\theta^{\mathrm{CFF}},\phi^{\mathrm{CFF}}$) rather than eight.

To properly isolate the desired variables, a curve fit was applied to the dipolar spectra of the single crystal L-alanine sample. The spectra were modeled by four pairs of Gaussian peaks, each symmetric about zero, located at $\pm\omega_{\mathrm{D}}^i$

$$\omega_{\mathrm{D}}^i = \omega_{\mathrm{D}}(\theta_i^{\mathrm{RFF}},\phi_i^{\mathrm{RFF}}) = \frac{\cos((\pi/2)\varphi)}{1-\varphi^2}4\sqrt{2}D\sin\theta_i^{\mathrm{RFF}} \times \cos\theta_i^{\mathrm{RFF}}\sin\phi_i^{\mathrm{RFF}}. \tag{10}$$

The values of θ^{RFF} and ϕ^{RFF} were replaced by functions defined by Eq. (9) making the value of ω_{D}^i dependent on the Euler angles and the CFF orientation. This allowed for all four peak pairs to be fit simultaneously by a single, defining orientation in the CFF.

Because the Euler angles also needed to be extracted from simulation, it was necessary to have more independent measurements. Therefore a series of REDOR experiments were carried out, that stepwise increase the initial rotational starting coordinate of the rotor period. This was accomplished via an adjustable time delay placed after the synchronizing trigger signal (∇) sent from the spinning controller, marking the beginning of a rotor period. Data sets with five different delays (n*10 μs for $\tau_r = 100$ μs) were collected, corresponding to $\phi^{\mathrm{RFF}} = x + n\pi/5$ (for $n = 0,1,2,3,4,5$). In terms of the CFF and the transformation matrix $\tilde{R}$, the increase in ϕ^{RFF} is equivalent to a decrease in the value of γ by π/5. One can then apply a global curve fit to all six spectra defined by $\gamma = \gamma_0 + n\pi/5$, for $n = 0$–5 using the same defining equations, the same variables α, β, γ, θ^{CFF}, and ϕ^{CFF}, with the only difference between the spectra being the value of n.

The fmins protocol, in the program Octave, was used to iteratively find the global minimum RMS difference between all six equations (again, all defined by the same values α, β, γ_0, θ^{CFF}, ϕ^{CFF}) and their six respective datasets simultaneously. These data and their corresponding global curve fit are shown in Figs. 5A–F. The results of this fit are compared in Table 1 with the literature (X-ray diffraction and neutron diffraction) CFF coordinates and the Euler angles measured by X-ray analysis of the single crystal sample showing excellent agreement. The accuracy of the curve fit is estimated by the RMS baseline noise level of the dipolar spectra, to be less then ±10 Hz. This gives a typical error of ±1° in the angular fits for these particular cases, but in a general case can range from <1° to 10° depending on the values of all five angular variables.

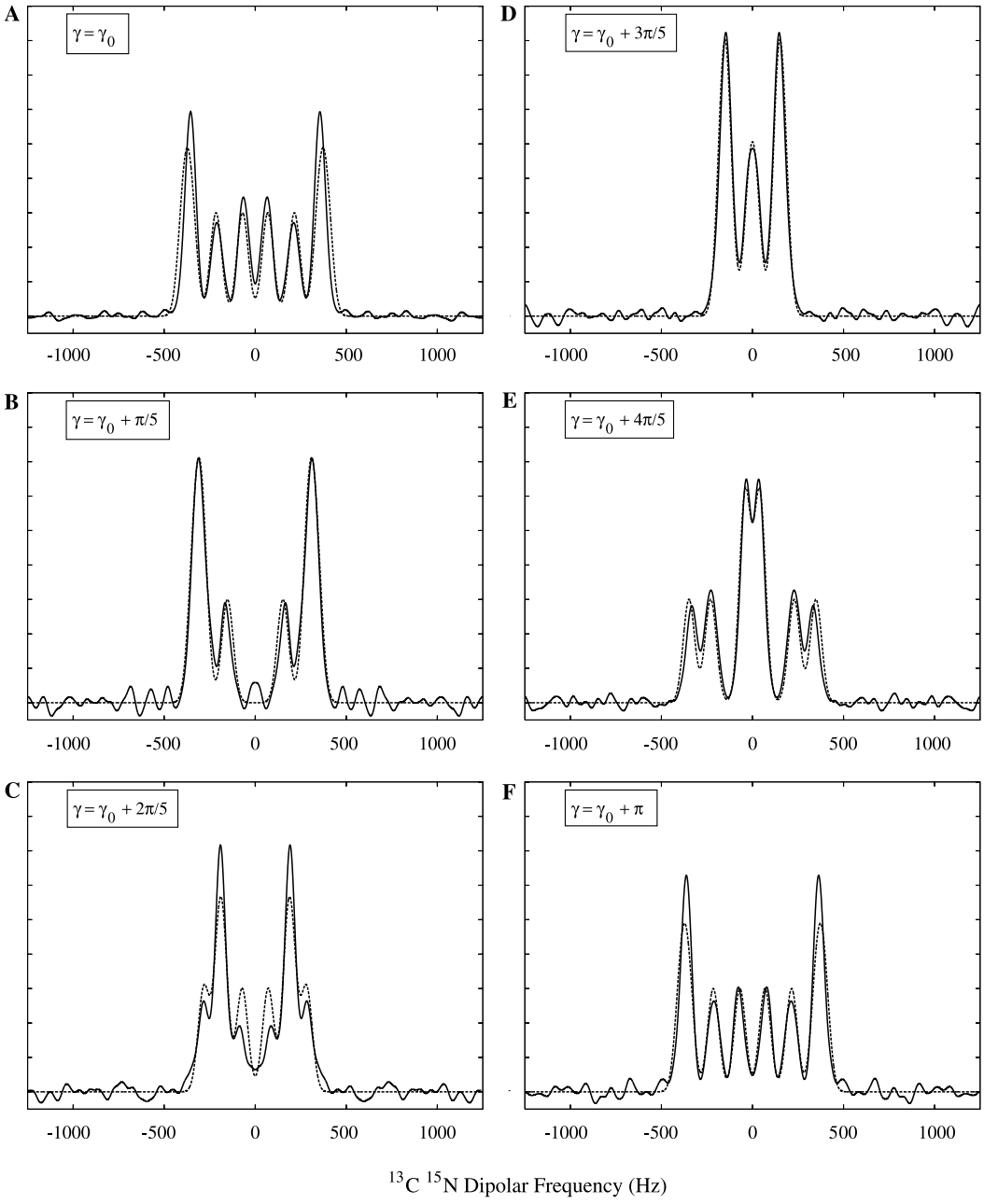

Fig. 5. ^{13}C–^{15}N REDOR detected dipolar spectra of the α carbon of single crystal L-alanine (solid line). These spectra were recorded at incremental initial azimuthal angles (γ) controlled by the delay (τ_d) between the rotational synchronizing trigger and the ^1H channel π/2 pulse. For (A) $\tau_d = 0$ μs, (B) $\tau_d = 10$ μs, (C) $\tau_d = 20$ μs, (D) $\tau_d = 30$ μs, (E) $\tau_d = 40$ μs, and (F) $\tau_d = 50$ μs with a sample spinning speed of 10,000 ± 5 Hz. The spectra were simultaneously curve fit to an expression based on Eq. (9 and 10) (dotted line) to find the best-fit values of α, β, γ_0, θ^{CFF}, and ϕ^{CFF}.

3.1. Uniaxially aligned system

For the system that simulated uniaxial alignment along the rotor axis, a different expression was used to extract the orientational data. The numerical expression for the REDOR curve is an integral over all azimuthal angles of the internuclear vector

$$\frac{\Delta S}{S_0} = 1 - \int_0^{2\pi} \cos\left(4\sqrt{2}n\tau_r D \sin\theta^{RFF}\cos\theta^{RFF}\sin\phi^{RFF}\right) \times d\phi^{RFF}. \quad (11)$$

Eq. (11) can be converted to a series of Bessel functions similarly to the powder formula, using the following relation

$$\cos(\xi\sin\phi) = J_0(\xi) + 2\sum_{k=1}^{\infty} J_{2k}(\xi)\cos(2k\phi), \quad (12)$$

where $\xi = 4\sqrt{2}n\tau_r D\sin\theta\cos\theta$. After integrating Eq. (12) over ϕ the only surviving component of this expression is the zero-order Bessel term

$$\frac{\Delta S}{S} = 1 - J_0\left(4\sqrt{2}n\tau_r D\frac{\cos((\pi/2)\varphi)}{1-\varphi^2}\sin\theta\cos\theta\right). \quad (13)$$

The long duration π-pulse modification from Eq. (6) was also implemented in Eq. (13). Comparison of Eq. (13) with a numerical integration of the general REDOR expression gives an appropriate match when a sufficiently large number of orientations are included. Under the experimental conditions used herein, 70 evenly spaced orientations were sufficient. Since the value of r (and thus D) had been determined, the only remaining variable to fit to experimental data was θ making Eq. (13) a direct calculation of the polar angle of the internuclear vector (in the RFF) of the dipolar pair under scrutiny. Fig. 3E shows the Fourier transform of this REDOR curve will result in a Pake-like pattern. Spectral analysis in general is practical here, since the splitting of the two main features of the generated spectrum will be equal to 2ξ. This allows for determination of the value of θ^{RFF} without the need for elaborate curve fitting techniques. However, since there were four orientations to decipher, a curve fit was used to isolate the individual values of θ^{RFF}. Fig. 6 shows a comparison of the fit values to the experimental dipolar spectrum. The results for θ_i^{RFF} are listed in Table 1 along with the single crystal data, and again show remarkable agreement.

It should be noted that of the three sample morphologies analyzed in this work, the uniaxially oriented sample was the easiest to obtain structural data from. It has a simpler expression for curve fitting, and were it not for the multiple orientations present in the spectrum, a simple measure of the wing splittings would give the dipolar coupling value of interest. It should further be noted that had the L-alanine crystal been aligned with its crystallographic axis coincident to the rotor axis, only one dipolar coupling value would have been exhibited, due to the unit cell symmetry. This would allow for the simplified analysis, provide the same amount of orientational data (assuming cubic symmetry), and is exactly the type of configuration anticipated for experiments on uniaxially aligned biological macromolecules.

Numerous approaches to fitting the REDOR data are applicable, depending on the sample type and degree of understanding one has of the sample prior to NMR analysis. The one assumption made consistently throughout this analysis is that the unit cell symmetry ($P_{2_12_12_1}$) is known. If one also were to assume the CFF to RFF transform Euler angles as being taken from an external measurement (such as X-ray indexing), it is readily possible to determine the CFF bond vector coordinates from a single REDOR experiment. This is a reasonable approach if one had a large single crystal sample that was of too poor quality for high resolution X-ray diffraction. If there are no characterizations other than the symmetry, and no other types of NMR experiments are to be performed, then multiple data sets will be needed for curve fitting. As in this study, the repeated addition of a known amount ($n\pi/5$) to one of the variables (γ) provided enough redundancy in the data set to allow complete determination of the $^{13}C_\alpha$–^{15}N bond vector orientation in the CFF, and the Euler angles defining the frame transform between CFF and RFF. All six spectra ($n = 0$–π) were compared in a global curve fit that simultaneously calculated the optimal values of α, β, γ_0, θ^{CFF}, and ϕ^{CFF} for maximum reliability. These

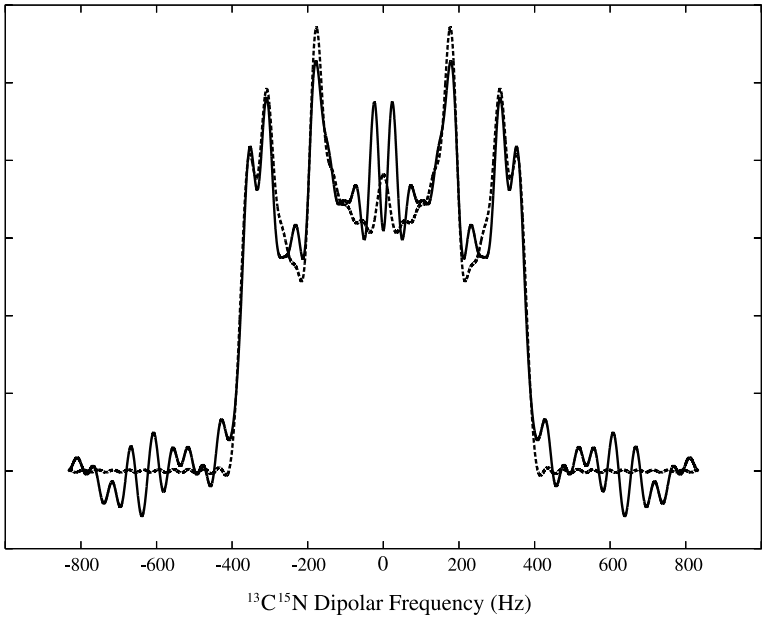

Fig. 6. The ^{13}C–^{15}N REDOR detected dipolar spectrum of the α carbon in the L-alanine single crystal sample, simulating a uniaxial alignment (solid line) fit to a spectrum generated by Eq. (13) (dashed line). The peak separations, symmetric about zero are indicative of the polar tilt angle (θ^{RFF}) of the internuclear vector. While the uniaxially aligned REDOR experiment does not provide complete bond orientations (θ^{CFF}, ϕ^{CFF}), it will be a more feasible method of studying biological macromolecular systems than the single crystal experiment of Fig. 5.

data are shown in Table 1. One could actually fit these values to as many experimental data sets as desired, but six seems a reasonable compromise between accuracy and experiment time.

In the extreme case where no other information about the sample is available, one can still gather useful, structural information from this REDOR data. Fitting each spectrum to four values of ω_d will give, for each value, a family of possible orientation coordinates. Even though this is not as dramatic an identifier as complete orientation determination, it remains a drastic constraint on an overall structure calculation. It should also be noted that were it possible to assign each ω_d value to a particular unit cell species throughout all six single crystal spectra, it would be possible to model, not only the RFF coordinates, but the symmetry relation $P_{2_12_12_1}$, and the Euler transform angles to get the CFF coordinates. This could be achieved by correlating the REDOR measured coupling to the specific $^1H^{13}C_\alpha$ coupling measurement (which would also be orientationally dependent) in an additional dimension.

If each dipolar coupling value were spectrally isolated, one could follow the change in $^{13}C_\alpha$–^{15}N dipolar coupling based on known changes in γ. This would be analogous to performing a REDOR experiment on a simulation of a uniaxially aligned sample (as performed herein) to determine θ^{RFF}, and then the only remaining variable would be ϕ^{RFF}, which could be determined by a single orientation REDOR measurement. As previously mentioned, this would be straightforward if the sample were aligned with its symmetry axis coincident to the rotor axis, as only one value would be measurable. The L-alanine crystal axes in this study were intentionally tilted away from being coincident to the rotor axis to display the potential for structure determination in samples where convoluted spectra would be unavoidable.

4. Conclusion

Chemical shift selective REDOR experiments performed on a uniformly labeled, single crystal sample can provide the absolute orientation of the crystal axes and $^{13}C_\alpha$–^{15}N bond vectors in the MAS rotor fixed frame of reference. By globally curve fitting a series of six REDOR dipolar spectra taken at unique initial azimuthal orientations of known difference, the spherical coordinates of the $^{13}C_\alpha$–^{15}N bond vector in the CFF as well as the Euler angles of the CFF to RFF transformation matrix were determined for uniformly labeled L-alanine. Each dipolar spectra contained four pairs of Gaussian peaks separated by the average dipolar coupling value for each of the four $^{13}C_\alpha$–^{15}N bond vector orientations of the $P_{2_12_12_1}$ unit cell. All of the REDOR data was in agreement with the coordinates generated by X-ray indexing of the L-alanine sample, and literature crystal structures.

An analytic expression was also derived (based on Mueller's powder expression) for a uniaxially oriented sample, and was successfully compared to a combination of single crystal REDOR spectra simulating a uniaxially aligned sample. This allowed for determination of the polar angle of the bond vector being studied, relative to the rotor axis. With the ability to generate aligned protein samples via membranes on stacked glass slides, or fixing an orientation under a magnetic field, this could prove to be a most valuable, and widely applicable method of protein structure determination.

Another method for uniaxial protein alignment that shows much potential for SSNMR is crystal growth under a strong magnetic field [31,32]. This type of alignment has been achieved for a number of diamagnetic proteins, but has not yet been applied to NMR studies. Such possibilities for widespread oriented sample preparation increase the potential utility for NMR experiments that can extract orientational data.

Acknowledgments

We thank Professor Gerard Parkin of Columbia University for expert advice and generous help with the diffraction control. This work was supported by a grant from the NSF, MCB 03 16248.

References

[1] T.A. Cross, J.R. Quine, Protein structure in anisotropic environments: development of orientational constraints, Concept Magn. Reson. 12 (2000) 55–70.
[2] J.R. Quine, T.A. Cross, Protein structure in anisotropic environments: unique structural fold from orientational constraints, Concept Magn. Reson. 12 (2000) 71–82.
[3] A. Ramamoorthy, S.J. Opella, 2-Dimensional chemical-shift heteronuclear dipolar coupling spectra obtained with polarization inversion spin-exchange at the magic-angle and magic-angle sample-spinning (Pisemamas), Solid State Nucl. Mag. 4 (1995) 387–392.
[4] F. Tian, Z. Song, T.A. Cross, Orientational constraints derived from hydrated powder samples by two-dimensional PISEMA, J. Magn. Reson. 135 (1998) 227–231.
[5] S.K. Straus, W.R.P. Scott, A. Watts, Assessing the effects of time and spatial averaging in N-15 chemical shift/N-15-H-1 dipolar correlation solid state NMR experiments, J. Biomol. NMR 26 (2003) 283–295.
[6] S.H. Park, A.A. Mrse, A.A. Nevzorov, M.F. Mesleh, M. Oblatt-Montal, M. Montal, S.J. Opella, Three-dimensional structure of the channel-forming trans-membrane domain of virus protein "u" (Vpu) from HIV-1, J. Mol. Biol. 333 (2003) 409–424.
[7] F.M. Marassi, S.J. Opella, Simultaneous assignment and structure determination of a membrane protein from NMR orientational restraints, Protein Sci. 12 (2003) 403–411.
[8] S.J. Opella, F.M. Marassi, J.J. Gesell, A.P. Valente, Y. Kim, M. Oblatt-Montal, M. Montal, Structures of the M2 channel-lining

segments from nicotinic acetylcholine and NMDA receptors by NMR spectroscopy, Nat. Struct. Biol. 6 (1999) 374–379.
[9] N. Tjandra, A. Bax, Direct measurement of distances and angles in biomolecules by NMR in a dilute liquid crystalline medium, Science 278 (1997) 1111–1114.
[10] N. Tjandra, J.G. Omichinski, A.M. Gronenborn, G.M. Clore, A. Bax, Use of dipolar H-1-N-15 and H-1-C-13 couplings in the structure determination of magnetically oriented macromolecules in solution, Nat. Struct. Biol. 4 (1997) 732–738.
[11] J.R. Tolman, J.M. Flanagan, M.A. Kennedy, J.H. Prestegard, Nuclear magnetic dipole interactions in field-oriented proteins—information for structure determination in solution, Proc. Natl. Acad. Sci. USA 92 (1995) 9279–9283.
[12] A. Peshkovsky, A.E. McDermott, Dipolar interactions in molecules aligned by strong AC electric fields, J. Magn. Reson. 147 (2000) 104–109.
[13] J.H. Prestegard, H.M. Al-Hashimi, J.R. Tolman, NMR structures of biomolecules using field oriented media and residual dipolar couplings, Q. Rev. Biophys. 33 (2000) 371–424.
[14] C. Glaubitz, A. Watts, Magic angle-oriented sample spinning (MAOSS): a new approach toward biomembrane studies, J. Magn. Reson. 130 (1998) 305–316.
[15] T.I. Igumenova, A.J. Wand, A.E. McDermott, Assignment of the backbone resonances for microcrystalline ubiquitin, J. Am. Chem. Soc. 126 (2004) 5323–5331.
[16] J. Pauli, M. Baldus, B. van Rossum, H. de Groot, H. Oschkinat, Backbone and side-chain C-13 and N-15 signal assignments of the alpha-spectrin SH3 domain by magic angle spinning solid-state NMR at 17.6 tesla, Chembiochem 2 (2001) 272–281.
[17] A. McDermott, T. Polenova, A. Bockmann, K.W. Zilm, E.K. Paulsen, R.W. Martin, G.T. Montelione, Partial NMR assignments for uniformly (C-13, N-15)-enriched BPTI in the solid state, J. Biomol. NMR 16 (2000) 209–219.
[18] D.A. Middleton, Z. Ahmed, C. Glaubitz, A. Watts, REDOR NMR on a hydrophobic peptide in oriented membranes, J. Magn. Reson. 147 (2000) 366–370.
[19] T. Gullion, J. Schaefer, Rotational-echo double-resonance Nmr, J. Magn. Reson. 81 (1989) 196–200.
[20] L.M. McDowell, J. Schaefer, High-resolution NMR of biological solids, Curr. Opin. Struct. Biol. 6 (1996) 624–629.
[21] M.S. Lehmann, T.F. Koetzle, W.C. Hamilton, Precision neutron-diffraction structure determination of protein and nucleic-acid components.1. Crystal and molecular structure of amino-acid L-alanine, J. Am. Chem. Soc. 94 (1972) 2657.
[22] R. Destro, R.E. Marsh, R. Bianchi, A low-temperature (23-k) study of L-alanine, J. Phys. Chem. 92 (1988) 966–973.
[23] C.P. Jaroniec, B.A. Tounge, C.M. Rienstra, J. Herzfeld, R.G. Griffin, Measurement of C-13-N-15 distances in uniformly C-13 labeled biomolecules: *J*-decoupled REDOR, J. Am. Chem. Soc. 121 (1999) 10237–10238.
[24] J.W. Eaton, GNU Octave, <http://www.octave.org/>, University of Wisconsin, 1998.
[25] C.P. Jaroniec, B.A. Tounge, J. Herzfeld, R.G. Griffin, Frequency selective heteronuclear dipolar recoupling in rotating solids: accurate C-13-N-15 distance measurements in uniformly C-13,N-15-labeled peptides, J. Am. Chem. Soc. 123 (2001) 3507–3519.
[26] G.A. Morris, R. Freeman, Selective excitation in Fourier-transform nuclear magnetic-resonance, J. Magn. Reson. 29 (1978) 433–462.
[27] K.T. Mueller, Analytic solutions for the time evolution of dipolar-dephasing Nmr signals, J. Magn. Reson. A 113 (1995) 81–93.
[28] C.P. Jaroniec, B.A. Tounge, C.M. Rienstra, J. Herzfeld, R.G. Griffin, Recoupling of heteronuclear dipolar interactions with rotational-echo double-resonance at high magic-angle spinning frequencies, J. Magn. Reson. 146 (2000) 132–139.
[29] D.A. Case, Calculations of NMR dipolar coupling strengths in model peptides, J. Biomol. NMR 15 (1999) 95–102.
[30] Y. Ishii, T. Terao, S. Hayashi, Theory and simulation of vibrational effects on structural measurements by solid-state nuclear magnetic resonance, J. Chem. Phys. 107 (1997) 2760–2774.
[31] J.P. Astier, S. Veesler, R. Boistelle, Protein crystals orientation in a magnetic field, Acta Crystallogr. D Biol. Crystallogr. 54 (1998) 703–706.
[32] G. Sazaki, E. Yoshida, H. Komatsu, T. Nakada, S. Miyashita, K. Watanabe, Effects of a magnetic field on the nucleation and growth of protein crystals, J. Cryst. Growth 173 (1997) 231–234.